Electron pair emission from surfaces: Intensity relations

F. O. Schumann, Y. Aliaev, I. Kostanovskiy, G. Di Filippo, Z. Wei, and J. Kirschner
Max-Planck-Institut für Mikrostrukturphysik, Weinberg 2, 06120 Halle, Germany
(Received 16 March 2016; revised manuscript received 16 May 2016; published 15 June 2016)

The emission of an electron pair upon single-photon absorption requires a finite electron-electron interaction. Therefore, double photoemission is a particularly sensitive tool to study the electron correlation in matter. This is supported by a recent theoretical work which predicts that the pair intensity is a direct reflection of the correlation strength. In order to explore the validity of this statement, we performed a study on a variety of materials. Among them are noble metals, transition metals, and insulators. The latter include transition metal oxides such as CoO and NiO which are also termed highly correlated. We find an increased pair emission rate of NiO and CoO compared to the metals which reach a factor of 10. We also discovered that an increase of the coincidence intensity is accompanied by an increase in the singles count rate. This demonstrates that the electron pair emission is an efficient process at surfaces contributing up to 15% to the single-electron emission in double photoemission. We performed also electron pair emission studies upon primary electron impact and find similar intensity relations.

DOI: 10.1103/PhysRevB.93.235128

I. INTRODUCTION

It is a well-known fact that a single photon can lead to the emission of an electron. This effect forms the basis of photoemission spectroscopy which has developed into a versatile tool to study the electronic properties of matter. It is also possible that a single photon leads to the emission of an electron pair in which case we talk about double photoemission (DPE). As a matter of fact, this pathway was already anticipated by Einstein in his seminal paper on the photoelectric effect [1]. A key feature of this effect is the requirement of a finite electron correlation for a nonvanishing DPE intensity [2,3]. This leads immediately to the suggestion that the pair emission intensity may depend on the strength of the electron correlation. A theoretical DPE study focused on this aspect by investigating a model system in which the correlation strength was determined by the term U within the Hubbard model [4]. It was found that the DPE intensity scales with the correlation strength.

From an experimental point of view, two difficulties arise. First, the parameter U is a theoretical concept and it is not straightforward to determine it solely from a measurement. Second, the correlation strength of matter can not be easily tuned. In order to make connection to the DPE calculation, we study a variety of materials which possess different properties in particular manifestations of the electron correlation.

The emergence of long-range magnetic order such as ferromagnetism or antiferromagnetism has its roots in the exchange interaction which stems from the Coulomb interaction between electrons modified by the Pauli exclusion principle. This interaction tends to align the magnetic moments on different atomic sites to be either parallel or antiparallel. As to whether the formation of a local magnetic moment is energetically favorable depends on the electronic band structure. The Stoner criterion states that a sufficiently high density of states at the Fermi level E_F causes the emergence of ferromagnetism. This explains why Co, Fe, and Ni are ferromagnets, while Pd is a paramagnet despite having the same number of d electrons as Ni. The calculation of the band structure can be successfully accomplished by the density functional theory within the local density approximation. However, the same concept applied to the description of transition metal oxides such as CoO and NiO fails because the insulating properties of these materials are not captured. These have their origin in the electron correlation. The necessary refinement of the theory requires to treat the electron correlation to a higher degree of sophistication leading to the LDA + U framework [5]. From this point of view, we may regard NiO and CoO as highly correlated materials. Metals such as Ag, Cu, V, and Pd do not display long-range magnetic order. With this in mind, we performed a DPE study on the aforementioned materials and demonstrate largely varying coincidence rates. NiO is the material with the highest rate; it is a factor of 10 larger than for the value for V which shows the lowest rate. Additionally, we discovered that an increase of the coincidence rate is accompanied by an increase of the "singles" rate. This is a manifestation that the pair emission is a likely event; for NiO we will show that 14% of the electron emission is via electron pairs.

More insight was gained by additional (e,2e) experiments, which we performed in parallel under the same experimental conditions as the DPE studies. This extends our previous (e,2e) studies to more materials [6,7]. We find very similar results in the (e,2e) experiments for the material dependence of the coincidence rates. We also observe that an increase of the coincidence rate is accompanied by an increase of the singles rate. For NiO, we find that 42% of the electron emission proceeds via pair emission. The microscopic origin of electron pair emission in (e,2e) is a collision between primary electron and a target electron. This is very different from the absorption of a photon by an electron pair. Furthermore, in the DPE process two electrons are missing in the sample, while in a (e,2e) process only one electron is missing. Despite these differences, it is remarkable that both techniques lead to very similar results in the intensity relations. This strongly suggests that despite the microscopic differences DPE and (e,2e) a tool is at hand which can assess the electron correlation strength in matter.

II. EXPERIMENTAL DETAILS

The details of the coincidence spectrometer have been described in more detail elsewhere [8–10]. Therefore, we recall

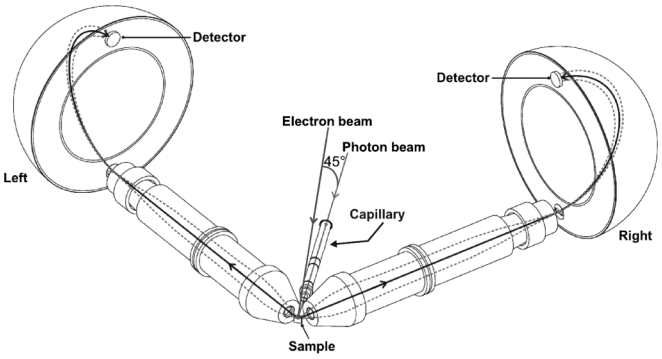

FIG. 1. The two transfer lenses of the spectrometer are symmetrically aligned with respect to the surface normal. The photon beam is aligned along the surface normal. An electron gun for (e,2e) experiments was available; this primary beam has an angle of 45° with respect to the scattering plane.

only the main aspects. The general layout in Fig. 1 shows two hemispherical electron energy analyzers with a mean radius of 200 mm. They are equipped with wide-angle transfer lenses and position-sensitive detectors. We label the spectrometers as "left" and "right," respectively. The two electron-optical axes of the transfer lenses include an angle of 90° and define the reaction plane, in which the primary photon beam lies. The emitted electrons are detected with energies E_{left} and E_{right}. Each transfer lens has an acceptance of ±15°. Due to the entrance slits, not all electrons which enter the lens will be detected. The orientation of the slits is such that the spectrometer will have a ±15° acceptance within the scattering plane. All experiments were performed with the photon beam being parallel to the normal. For additional (e,2e) experiments, an electron gun was available. The primary electron beam had an angle of 45° with respect to the scattering plane (see Fig. 1). For in-house experiments, the system has been upgraded by the attachment of VUV light source which consists of a He lamp [11] and a toroidal monochromator [12]. We used the He lines at 23.7, 40.8, and 48.4 eV, respectively. Space constraints do not allow to have the sample at the focus point of the grating. Therefore, we fitted the exit arm of the monochromator with an additional capillary of 200-mm length and 2-mm diameter. This has the added benefit of improved differential pumping. The partial pressure of He during normal operation is 2×10^{-10} mbar range, while the base pressure was 5×10^{-11} mbar. In order to reduce the primary flux on the sample, we placed a set of apertures between the He light source and the monochromator.

While the single-electron count rate can be readily read, the determination of the coincidence count rate is in principle more involved. In our coincidence experiment we are interested in those events in which a single photon leads to the emission of an electron pair, which we term "true" coincidences. However, it is also possible that two photons lead to the individual emission of single electrons which will be recorded by the coincidence electronics. These unwanted events are usually termed "random" coincidences. The "true" coincidences scale linearly with the primary flux, while the random contribution scales quadratically. This allows us to reduce the latter to an acceptable level. This comes at the expense of a low coincidence count rate. Following standard procedures documented in the literature we are able to remove the aggregate effect of the random coincidences [13,14]. The implementation of these procedures within our coincidence spectrometer has been explained in detail previously [10]. At this point, we can state that we are able to determine the true coincidence rate and energy spectra. Despite the operation with a low primary flux it takes only about 1 h of data acquisition to determine the true rate with sufficient statistics.

We operated the spectrometer with a pass energy of 150 eV which results in an energy window of 13 eV, which can be covered with each spectrometer. The slit size selected was 3.5 mm; this leads to an energy resolution of 0.9 eV. The linewidth of the VUV light (a few meV) or of the primary electron gun (0.3 eV) makes only a minor contribution. In contrast to the usual operation of electron spectrometer in which the kinetic energy is scanned, we fix all voltages of the electron-optical components for a given coincidence experiment.

Two four-pocket and two single-pocket evaporation sources were available. They were loaded with V, Fe, Ni, Co, Cu, and Pd high-purity charges. Via a load-lock system we could change the substrate material. The preparation of the Ag(100) surface followed standard procedures of Ar^+ sputtering and annealing. All experiments were performed at room temperature. For sample characterization equipment for Auger spectroscopy and low-energy electron diffraction were available. The preparation of NiO and CoO films on a Ag(100) substrate is well documented [15–21]. We evaporated Ni and Co in an oxygen atmosphere of 10^{-6} mbar. We also investigated a KCl(100) single crystal which was cleaned by heating to 420 K.

The key aspect of this work relates to intensity relations between different materials. This requires stable experimental conditions. The He light source was stable during operation, but we found daily variation of its intensity upon startup each morning. In order to compensate for this, we executed the experiment as follows. Each day we began with the study of a freshly prepared Ag(100) surface and determined the singles and the true coincidence rates. This measurement was followed by the preparation of the various films while the VUV source was kept running. The count rates of these samples were recorded. In a next step, we divided these values with those of the Ag(100) surface at the beginning of the day. This gives normalized count rates for each material measured at a given day. These values are independent of the primary flux. These types of measurements have been repeated and we will report on the average of the normalized data. In order to confirm the stability during the daily routine, each experimental run included also a Pd film. This allowed us to compute the average ratio of the Pd to Ag count rates for all measurements. It was found that the daily Pd to Ag ratio was in agreement with the average ratio. This confirms the daily stability of the instrument.

We adjusted the primary flux such that the ratio of true to random events was approximately 9 for Ag for the DPE and (e,2e) experiments. This lead to a singles rate of 1200 cps while the true rate was 0.52 cps in the case of the DPE experiment on Ag. In the case of (e,2e) on Ag we determined a singles and true rate of 3950 and 4.2 cps, respectively. These low count rates are a consequence of the low primary flux.

III. RESULTS AND DISCUSSION

If a photon is absorbed by a surface electron emission will occur with a certain probability which is material and photon energy dependent [22]. A conceptional simple approach to quantify this is the measurement of the sample current to ground. In this way, one integrates over all possible emission angles and energies. If the photon flux is known, one can derive the average number of emitted electrons per incoming photon. This value is known in the literature as total electron yield (TEY) [23,24].

A numerical example for a Au surface at $h\nu = 50$ eV is TEY = 0.07 [24]. We can interpret this value in two ways. If we assume only single-electron emission, roughly 14 photons are required for one emitted electron. On the other hand, if only electron pairs are emitted, then 28 photons are needed to result in the emission of one electron pair. Both scenarios result in the same value of the TEY. In any real material, the electron emission will have contributions from both paths and only via coincidence spectroscopy one can disentangle them.

A photoemission spectrum can be qualitatively sketched as seen in Fig. 2. We assume a photon energy of 40.8 eV and a work function of 4.6 eV of some metallic surface. For simplification, we suppose that the photon energy is not sufficient to excite core levels and subsequent Auger electron emission is not present. This condition is fulfilled in our experiments. In this case, the spectrum displays two regions of high intensity at the high- and low-energy sides. At low kinetic energies, the emission is ascribed to secondary electrons and the shape for most materials is such that the intensity has a peak around 2–3 eV with a width of say 4 eV [25]. At the high-energy side, the spectrum has a cutoff and the electrons with the highest kinetic energy are due to single-electron emission from the Fermi level. A typical valence bandwidth is of the order of 5–10 eV, hence, the emission near E_F within a window of this size is usually ascribed to as single-electron emission. This

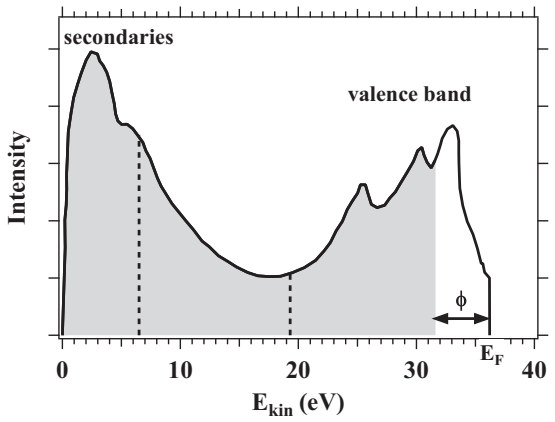

FIG. 2. Schematic single-electron photoemission spectrum obtained with the He II_α line at $h\nu = 40.8$ eV. The metal is supposed to have a work function $\phi = 4.6$ eV. Two regions of high intensity and both ends of the spectrum are referred to as secondary or valence band emission, respectively. The gray shaded part of the spectrum indicates where the detected electron could have a counterpart. The dashed vertical lines mark the energy spectrum which our spectrometer covers during the coincidence measurements at $h\nu = 40.8$ eV.

picture forms the basis of band mapping via angle-resolved photoemission. However, double photoemission from surfaces is a given fact [14,26–33]. Therefore, the single-electron spectrum will have contributions from double photoemission. Suppose the emission consists of the ejection of an electron with zero kinetic energy which is not detected by the spectrometer. The counterpart is recorded by the spectrometer and energy conservation will determine the maximum energy of this electron. The value is $h\nu$-2ϕ in contrast to the single photoemission cutoff at $h\nu$-ϕ. We visualized this in Fig. 2 by a gray shaded region in which DPE events make a contribution to the intensity. Only the narrow white part of the spectrum is solely due to single-electron emission. If such a large part of the spectrum is affected by pair emission, the question arises about its intensity level. In our experiment, we use a pair of electron spectrometers which cover an energy window given by the pair of dashed vertical lines in Fig. 2. The width is about 9% of the selected pass energy, which amounts to 13 eV in this work. The chosen central energy of the spectral range is roughly half of $h\nu$-2ϕ which ensures that most of the pair intensity is covered. This can be judged by the two-dimensional (2D) energy distributions to be presented below. The key point is to note that the part of the spectrum which usually ascribed to valence band photoemission is not captured by our settings (see Fig. 2). In Fig. 3, we present the 2D energy distributions from a Ag(100) surface and a 10-ML-thick NiO/Ag(100) film. The photon energy was set to 40.8 eV. In each of the two panels, we added a diagonal line. This marks the maximum energy an electron pair can have, it is given by $h\nu$-2ϕ. As expected from energy conservation, there is no intensity above the diagonal lines apart from some contributions from "random" coincidences. Both spectra are also slightly asymmetric despite the fact that the emission geometry is symmetric. We associate this to the difficulty to align the transfer lenses of the spectrometer onto the same spot on the sample. Both spectra display rather broad features which we can tentatively understand if we recall some facts on the Auger decay involving valence states. In such a decay, two electrons are missing in the valence band as in our DPE experiments. A sophisticated theory which describes the Auger line shape has been developed by Cini and Sawatzky [34,35]. In the limit of an electron correlation parameter U which is much smaller than the valence band width, this framework reduces to a self-convolution of the single-electron density of states [36]. The effect of the electron correlation parameter causes a distortion of the self-convolution such that spectral width is moved to lower kinetic energies of the Auger line. This means in a first approximation we expect rather featureless energy spectra. Investigations with improved energy resolution are in progress to address the details of the energy distributions.

In the following, we want to discuss the intensity integrated over the measured 2D energy spectra obtained for the various samples. As discussed in the experimental section, we quote the singles and true rates of each material normalized to the values of the Ag substrate. For this reference material we recorded a singles and true rate of 1200 and 0.52 cps, respectively.

In Fig. 4(a), we show the material dependence of the normalized rates for $h\nu = 40.8$ eV. The material with the lowest singles rate is V which has a value almost a factor

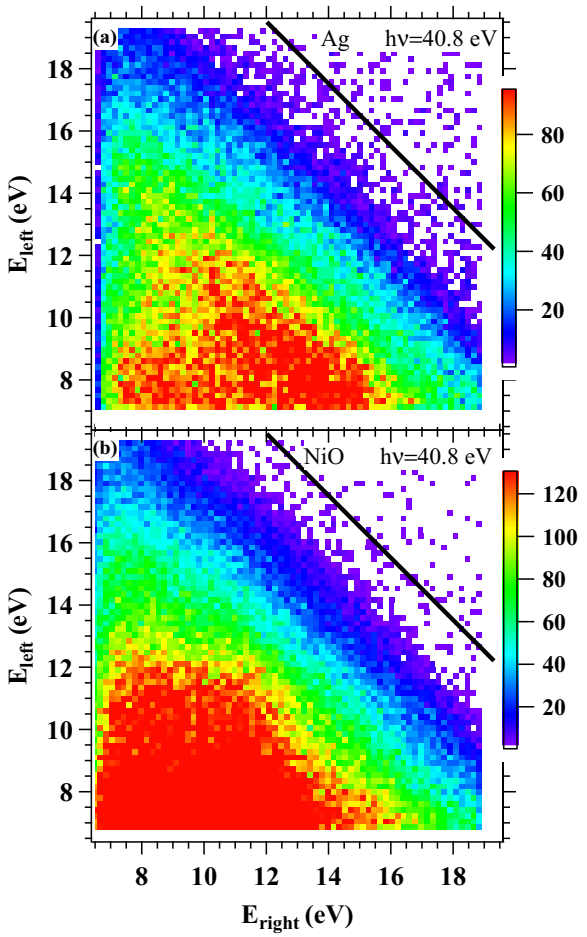

FIG. 3. 2D energy distributions of the DPE experiment with hν = 40.8 eV are presented. In (a) we show the result for the Ag(100) surface while in (b) the data for 10 ML NiO/Ag(100) are displayed. The solid diagonal line marks the maximum value of the energy sum of a pair. This value is given by hν-2ϕ.

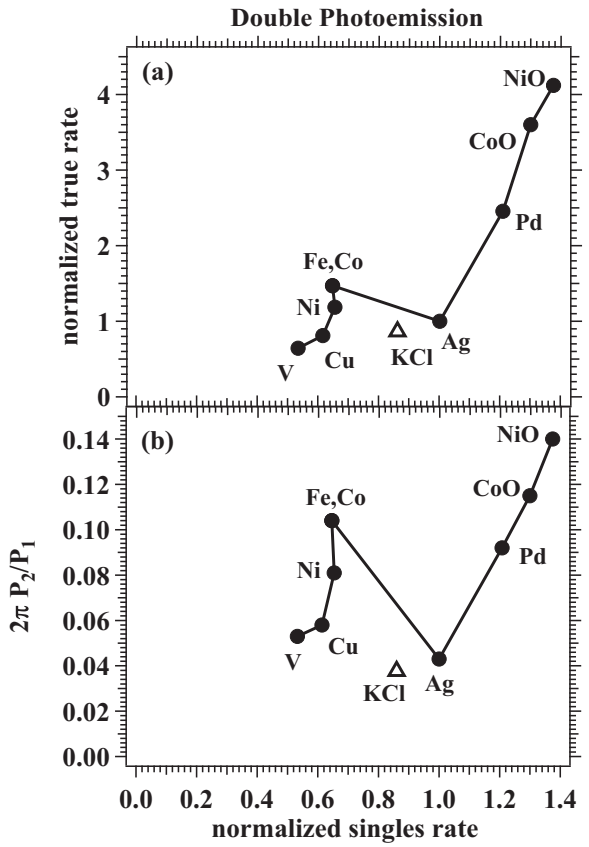

FIG. 4. In (a), we plot the normalized true rate as a function of the normalized singles rate following a procedure explained in the text. The photon energy was 40.8 eV. The data point for the KCl(100) surface was obtained at 48.4 eV. In (b), we show the variation of the dimensionless term $2\pi P_2/P_1$ [see Eq. (3)]. For the reference material Ag, we find a singles and true rate of 1200 and 0.52 cps, respectively.

of 3 smaller than the corresponding value for NiO. At the same time, the true rate of NiO reveals an enhancement of roughly a factor of 8 compared to V. This means that the inelastic part of the singles spectrum which we cover by our spectrometers contains a large fraction of electron pairs. If we ignore the data points for Fe, Co, and Ni for the moment, one can state we observe an almost monotonic variation of the coincidence rate as a function of the singles rate. More importantly, the transition metal oxides NiO and CoO display the highest true rate. We regard this as a manifestation of the theoretical prediction that the pair emission rate scales with the electron correlation strength [4]. An important point is also the measurement on a KCl single-crystal surface. The work function of the Ag(100) surface is 4.64 eV, the equivalent value for KCl is 8.5 eV [37]. In order to have the same kinematics, it is necessary to increase the photon energy by 7.7 eV because the additional energy has be supplied twice. Therefore, we changed from the 40.8 eV to the 48.4 eV line, which almost exactly amounts to the required increase. The acquired energy spectrum revealed that a significant part was not captured with the spectrometer settings, therefore, we lowered the central energy of both spectrometers slightly. KCl is an insulator like NiO or CoO, but does not possess the intensity level of these oxides. This means the higher intensity level of NiO and CoO is a reflection of the stronger electron correlation in this material rather than its insulating properties. This is of relevance because it could have been argued that the longer mean-free path of electrons in an insulator increases the number of layers probed by in a DPE experiment. Obviously, this mechanism is not responsible for the enhanced intensity levels of NiO and CoO.

Coming back to the ferromagnetic samples, we note that they display about 65% of the Ag singles rate, but possesses up to a factor 1.5 higher true rate. This means that the ratio of the true rate to the singles rate is significantly higher than for Ag. The question arises as to what meaning one can give to this ratio.

For a further discussion, it is worthwhile to make the following definitions. The probability for one electron to be emitted within a solid angle interval ranging from Ω to $\Omega + d\Omega$ is given by $P_1(\Omega)d\Omega$. For pair emission, we introduce the term $P_2(\Omega_A,\Omega_B)d\Omega_A d\Omega_B$. This describes the joint probability that one electron is emitted in a solid angle range centered at Ω_A while the other electron emission direction is characterized by Ω_B. We emphasize that in our definition the term $P_1(\Omega)d\Omega$

includes also electron pair excitation, but the second electron never escapes the surface.

In previous publications, we have discussed the angular distributions of electron pairs in the context of the exchange-correlation hole [31,32,38,39]. We found in DPE and (e,2e) experiments that the electrons tend to avoid to have the same emission direction. The pair intensity increases once the difference in the emission angles increases. It turns out that the angle-averaged value of the pair intensity is roughly obtained for emission directions captured by the current setup. The same is true for the angular distribution of single electrons. This means the simplification to use angular-averaged values of the functions P_1 and P_2 can be justified. For the probability s to detect one electron, we can write

$$s = \int (P_1 + 2\pi P_2) d\Omega_A = P_1 \left(1 + \frac{2\pi P_2}{P_1}\right)\Omega. \qquad (1)$$

As stated above, the single-electron detection has contributions from single-electron emission and pair emission. The factor of 2π in front of the term P_2 reflects the fact that the second (but undetected electron) is emitted somewhere within the half-sphere. The transfer lens accepts electrons within a cone with an opening angle of 15°. This amounts to a solid angle of 3.4% of 2π. The entrance slits will limit electrons entering the hemisphere. We simulated the electron trajectories within the transfer lens and slit assembly [40]. We find that the angular acceptance of the spectrometer for 3.5-mm slits is 1% of 2π. Hence, we use this value for Ω in our evaluations. The probability t to detect an electron pair can be formulated. We assume an operation with two identical spectrometers:

$$t = \int P_2 d\Omega_A d\Omega_B = P_2 \Omega^2. \qquad (2)$$

Our goal is to derive a relation between the probabilities P_1 and P_2. This is possible from Eqs. (1) and (2); we obtain after some simple rearrangements the following relation:

$$\frac{2\pi P_2}{P_1} = \frac{2\pi}{\Omega \cdot s/t - 2\pi} \approx \frac{2\pi}{\Omega}\frac{t}{s}. \qquad (3)$$

The term $2\pi P_2/P_1$ is dimensionless and gives the additional contribution of pair emission to the detected single-electron spectrum [see Eq. (1)]. The factor 2π emphasizes that the second (undetected) electron is emitted somewhere in the half-space. The ratio s/t is identical to the experimentally determined ratio of singles and true coincidence count rate. For the experiments on Ag(100), we find a ratio of 2400. The solid angle of our spectrometer is about 1% of 2π as discussed above. This means the denominator is essentially given by the first term and it turns out that the ratio of true to the singles rate determines the fraction of the pairs to the singles rate. Nevertheless, we will use the exact expression in the following.

The evaluation of the experimental data via Eq. (3) leads to Fig. 4(b). It displays the term $2\pi P_2/P_1$ as a function of the normalized singles rate. We see that this curve resembles Fig. 4 in the shape, but demonstrates the interesting point that 5%–15% of the singles emission is due to pairs. This means that DPE at surfaces is a rather efficient process. In the presentation of Fig. 4(b), the signal levels of the ferromagnets Fe, Co, and Ni are significantly higher than Ag. This is a reasonable result because ferromagnetism is a manifestation of electron correlation. This suggest that the term $2\pi P_2/P_1$ may be better suited for the quantification of the correlation strength.

In a previous study, we also discovered similar intensity relations in the (e,2e) process from NiO, CoO, and metallic Co and Ni films [7]. In that work, the primary energy was $E_p = 32$ eV and a normal incidence primary electron beam. In the course of the present DPE study, we also performed (e,2e) in an interleaved mode covering a larger number of samples than before. As indicated in the sketch of Fig. 1, the primary electron beam was inclined by 45° with respect to the scattering plane. In the energy balance of the (e,2e) experiment, the work function of the sample enters only once in contrast to DPE. Therefore, we selected as primary energy $E_p = 36$ eV, which is 4.8 eV smaller than the photon energy used for the experimental data presented in Fig. 4. After the completion of a DPE measurement on a given sample, the photon beam was blocked and a primary electron beam was focused on the sample. This ensured that the spectral features are captured without the need to change the spectrometer settings. The time required to obtain the relevant intensity levels is about an hour. This means during the DPE and (e,2e) experiments, the sample properties are not affected.

The intensity relations for the (e,2e) measurement are presented in Fig. 5 as a function of the normalized singles rate in analogy to the DPE data shown in Fig. 4. We adjusted the primary flux such that the ratio true to random obtains 9 for Ag which is the same value as for the DPE measurements on Ag. This choice ensures the same coincidence conditions for the two types of experiments. This leads to a (e,2e) singles and true rate for Ag of 3950 and 4.2 cps, respectively. This means compared to the DPE experiments the true rate is about 8 times larger in (e,2e) while the singles rate is about a factor of 3 larger. The highest coincidence rate is observed for NiO which is about a factor 6 larger than for Ag while the singles rate is a factor of 2 larger than for Ag. Furthermore, the variation of the singles and true rates for all materials covers a larger range than for the DPE measurement. In the presentation of the data in Figs. 4 and 5, the knowledge of the constant primary flux of electrons and photons is not required. First, the singles and the true rates are proportional to the flux. Furthermore, for the evaluation of the term $2\pi P_2/P_1$, only the ratio of singles to the true rate is needed [see Eq. (3)]. It is of course highly desirable to be able to quantify the primary flux. During the course of these studies, we were not able to do this. The significant different rates in (e,2e) lead to larger values of the term $2\pi P_2/P_1$ as seen in Fig. 5(b). For NiO, we find that the additional contribution of pairs to the singles rate amounts to 42% in (e,2e) while in the DPE study we found a value of 14%. In contrast to the DPE case shown in Fig. 4(b), the term $2\pi P_2/P_1$ does not display a marked increase for Fe, Co, and Ni compared to Cu or Ag. This is related on how the two techniques probe the initial state correlation as we will discuss below.

We recall that the number of emitted electrons per incoming particle is largely different for photons and electrons. For 50-eV photons, the total electron yield is about 0.06 for the metals studied by us [24,41]. For the yield due to electron excitation, we obtain values of about 0.4 at a $E_p = 36$ eV for

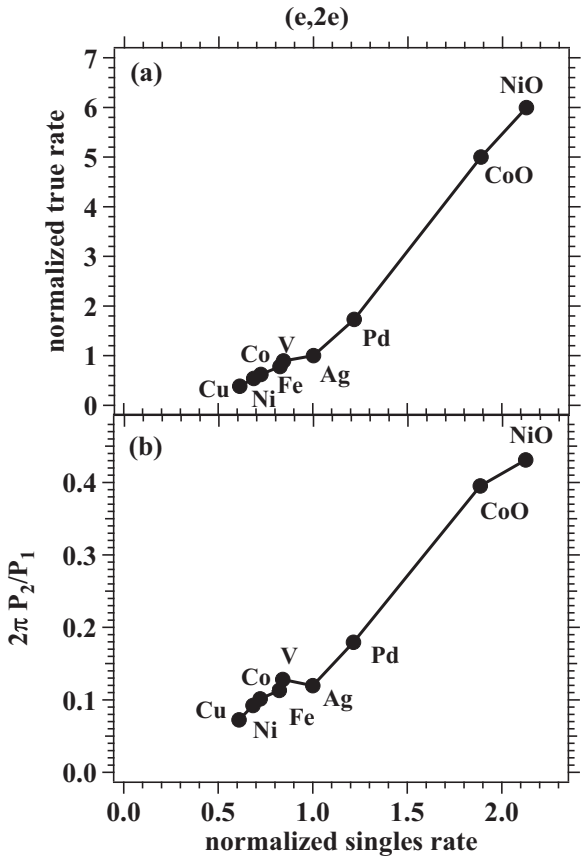

FIG. 5. In (a), we plot the normalized true rate as a function of the normalized singles rate following a procedure explained in the text. The primary electron energy was $E_p = 36$ eV. In (b), we show the variation of the dimensionless term $2\pi\, P_2/P_1$ [see Eq. (3)]. For the reference material Ag we find a singles and true rate of 3950 and 4.2 cps, respectively.

most of the studied metals [42]. An effect contributing to this observation is related to the larger penetration depth of photons into the surface compared to low-energy primary electrons. This means on average photoexcited electrons have to traverse a larger distance before they escape the surface, compared to electrons excited in an electron-electron collision event. The detection of electron pairs will enhance the surface sensitivity further. These simple arguments explain the larger variation of the singles and coincidence rates in (e,2e). Recently, CoO and NiO films were in the focus of electron pair emission studies in which the $3p$ Ni or Co $3p$ photoelectron was detected in coincidence with Auger decay electron [43–46]. These studies employed two experimental geometries, and it was found that the Auger line shape was different in the two measurements. This dichroism was found to vanish at the Néel temperature of the films. Clearly, these studies reveal a dependence on the long-range order. We have addressed this point in a previous (e,2e) study on NiO/Ag(100) films and found no variation in the count rates above and below the Néel temperature [7]. We repeated this for the DPE process and found also no variation in the count rates. This proves that the DPE without participation of core levels is not sensitive to the long-range order, but probes the local correlation. We point out that an enhanced coincidence rate for NiO compared to Ag was also observed for positron-electron pair emission as presented recently [47,48]. Despite the fact that the process leading to the emission of the pairs is largely different, it is remarkable that the coincidence intensity for NiO is largest for all experiments.

In order to work out the basics of the pair emission process at surfaces, it is useful to discuss a system which contains only two electrons, e.g., the He atom. If there is no Coulomb interaction between the two electrons, the Hamiltonian is simply the sum of two single-electron Hamiltonians which commute. Therefore, the two-electron wave function is a product of single-electron wave functions. Adding the Coulomb interaction between the electrons has the consequence that the single-electron Hamiltonian does not commute with the electron interaction term. Hence, the exact two-electron wave function cannot have the form of products of single-electron wave functions. It must contain a term which depends on the coordinate difference of the two electrons.

Nevertheless, it is possible to approximate the two-electron wave function via a product of single-electron wave functions. For example, we may use hydrogen-type wave functions in which the charge $Z = 2$ of the nucleus is being replaced by $\tilde{Z}$. This takes into account the screening of the nucleus charge due to the presence of the other electron. The term $\tilde{Z}$ can be treated as a parameter in a variational scheme, and the obtained ground-state energy or double-ionization energy is only 2% higher than the experimental value [49]. This means an effective single-electron picture can provide a good description of electronic states in the presence of electron correlation.

In quantum mechanics textbooks, the absorption of light is discussed. In Ref. [2], we quote a textbook which goes a step further [2]. It is shown that if a photon is absorbed by a many-electron system which is described by single-electron wave functions, only the state of one electron is changed. Coming back to the He atom, it means that an effective single-electron picture, despite the inclusion of electron correlation, cannot explain the DPE process. On the other hand, there is clear experimental evidence that a single photon can yield He^{2+} ions, which means two electrons have been emitted. Hence, for a theoretical treatment, the initial state has to be described beyond an effective single-electron picture. This means the initial state correlation has to be properly incorporated. The minimum requirement is a two-electron wave function which explicitly depends on the coordinate difference [50]. The basic ingredient in a (e,2e) process is the collision of the incoming electron with a valence electron. The approximation of a single-electron picture for the valence state will lead to a finite (e,2e) intensity. We learn from this discussion that the DPE process requires a more accurate description of the electron correlation. In this sense, the DPE process is more sensitive to the initial state correlation than the (e,2e) process.

An effective single-particle (or quasiparticle) description of matter is the local density approximation of the density functional theory [51,52]. It is a powerful tool capable to predict material properties rather accurately. The aspect of the interaction between the electrons is cast into the exchange-correlation functional. This term shows up as a potential energy term in the Kohn-Sham equation which is in a formal sense a single-electron Schrödinger equation. Using these

quasiparticle states will not yield a finite DPE intensity. Consequently, the theory of DPE has to include an implicit interaction between two electrons [3,53,54]. At the heart of the (e,2e) process is the collision of the primary electron with a valence band electron. Hence, the electron-electron interaction between these two electrons is the perturbation to the system. The response of an electronic system to some external electric field is determined by the dielectric function which itself depends on the electron correlation. Therefore, the valence electron will not experience the bare Coulomb interaction of the incoming electron, but a screened Coulomb interaction. Current (e,2e) calculations employ a Thomas-Fermi screening [53–60].

The reasoning used in the He atom case as to why DPE is more sensitive to the initial state correlation than the (e,2e) process survives in the description of pair emission of surfaces. This explains the increased normalized DPE intensity of the ferromagnets compared to (e,2e) [see Figs. 4(b) and 5(b)].

IV. SUMMARY

We performed DPE experiments on a variety of materials. We found a marked increase of the intensity levels for NiO and CoO compared to the Ag(100) surface and other metals. This is not caused by the insulating properties of NiO and CoO as a comparison with the data of the KCl(100) surface reveals. Our results also demonstrate that there exists a relation between the singles count rate and coincidence rate. In simple terms, one can say that the higher the singles rate is, the higher the coincidence rate becomes. An estimate shows that double photoemission is an efficient process because 4%–14% of the detected electrons in one spectrometer have a counterpart emitted somewhere in the half-sphere. We also performed (e,2e) experiments on the sample materials under identical experimental conditions. We found an almost monotonic relation between the singles and coincidence rates which is very similar to the feature observed in DPE. Again, NiO is the material with the highest coincidence rate which in the (e,2e) case reveals a pair contribution to the singles rate of 42%. Our presented work together with recently published data on positron-electron pair emission [47,48] provide a firm basis that the electron pair emission holds the power to assess the correlation strength of matter.

ACKNOWLEDGMENTS

We benefited from stimulating discussions with J. Berakdar and Y. Pavlyukh. Funding from the DFG through Grant No. SFB 762 is gratefully acknowledged.

[1] A. Einstein, Ann. Phys. **322**, 132 (1905).
[2] J. L. Powell and B. Crasemann, *Quantum Mechanics* (Addison-Wesley, Reading, MA, 1961).
[3] J. Berakdar, Phys. Rev. B **58**, 9808 (1998).
[4] B. D. Napitu and J. Berakdar, Phys. Rev. B **81**, 195108 (2010).
[5] V. I. Anisimov, J. Zaanen, and O. K. Andersen, Phys. Rev. B **44**, 943 (1991).
[6] F. O. Schumann, L. Behnke, C. H. Li, J. Kirschner, Y. Pavlyukh, and J. Berakdar, Phys. Rev. B **86**, 035131 (2012).
[7] F. O. Schumann, L. Behnke, C. H. Li, and J. Kirschner, J. Phys.: Condens. Matter **25**, 094002 (2013).
[8] G. A. van Riessen, F. O. Schumann, M. Birke, C. Winkler, and J. Kirschner, J. Phys.: Condens. Matter **20**, 442001 (2008).
[9] G. A. van Riessen, Z. Wei, R. S. Dhaka, C. Winkler, F. O. Schumann, and J. Kirschner, J. Phys.: Condens. Matter **22**, 092201 (2010).
[10] F. O. Schumann, R. S. Dhaka, G. A. van Riessen, Z. Wei, and J. Kirschner, Phys. Rev. B **84**, 125106 (2011).
[11] Light source MBS L-1 from MB Scientific.
[12] Monochromator VUV5040 from VG Scienta.
[13] G. A. Sawatzky, Auger photoelectron coincidence spectroscopy, in *Auger Electron Spectroscopy*, edited by C. L. Bryant and M. P. Messmer (Academic Press, San Diego, 1988).
[14] E. Jensen, R. A. Bartynski, S. L. Hulbert, and E. Johnson, Rev. Sci. Instrum. **63**, 3013 (1992).
[15] S. Peacor and T. Hibma, Surf. Sci. **301**, 11 (1994).
[16] J. Wollschläger, D. Erdös, H. Goldbach, R. Höpken, and K. M. Schröder, Thin Solid Films **400**, 1 (2001).
[17] S. Grosser, C. Hagendorf, H. Neddermeyer, and W. Widdra, Surf. Interface Anal. **40**, 1741 (2008).
[18] M. Caffio, B. Cortigiani, G. Rovida, A. Atrei, C. Giovanardi, A. di Bona, and S. Valeri, Surf. Sci. **531**, 368 (2003).
[19] K. Marre and H. Neddermeyer, Surf. Sci. **287-288**, 995 (1993).
[20] K. Marre, H. Neddermeyer, A. Chassé, and P. Rennert, Surf. Sci. **357-358**, 233 (1996).
[21] K.-M. Schindler, J. Wang, A. Chassè, H. Neddermeyer, and W. Widdra, Surf. Sci. **603**, 2658 (2009).
[22] J. J. Yeh and I. Lindau, At. Data Nucl. Data Tables **32**, 1 (1985).
[23] R. B. Cairns and J. A. R. Samson, J. Opt. Soc. Am. **56**, 1568 (1966).
[24] H. Henneken, F. Scholze, and G. Ulm, J. Appl. Phys. **87**, 257 (2000).
[25] B. L. Henke, J. Liesegang, and S. D. Smith, Phys. Rev. B **19**, 3004 (1979).
[26] H. W. Haak, G. A. Sawatzky, and T. D. Thomas, Phys. Rev. Lett. **41**, 1825 (1978).
[27] C. Gazier and J. Prescott, Phys. Lett. A **32**, 425 (1970).
[28] R. Herrmann, S. Samarin, H. Schwabe, and J. Kirschner, Phys. Rev. Lett. **81**, 2148 (1998).
[29] H. W. Biester, M. J. Besnard, G. Dujardin, L. Hellner, and E. E. Koch, Phys. Rev. Lett. **59**, 1277 (1987).
[30] E. Jensen, R. A. Bartynski, S. L. Hulbert, E. D. Johnson, and R. Garrett, Phys. Rev. Lett. **62**, 71 (1989).
[31] F. O. Schumann, C. Winkler, G. Kerherve, and J. Kirschner, Phys. Rev. B **73**, 041404(R) (2006).
[32] F. O. Schumann, C. Winkler, and J. Kirschner, Phys. Rev. Lett. **98**, 257604 (2007).
[33] F. O. Schumann, C. Winkler, and J. Kirschner, Phys. Status Solidi B **246**, 1483 (2009).
[34] M. Cini, Solid State Commun. **24**, 681 (1977).
[35] G. A. Sawatzky, Phys. Rev. Lett. **39**, 504 (1977).

[36] J. J. Lander, Phys. Rev. **91**, 1382 (1953).
[37] R. T. Poole, J. G. Jenkin, J. Liesegang, and R. C. G. Leckey, Phys. Rev. B **11**, 5179 (1975).
[38] F. O. Schumann, J. Kirschner, and J. Berakdar, Phys. Rev. Lett. **95**, 117601 (2005).
[39] F. O. Schumann, C. Winkler, and J. Kirschner, New J. Phys. **9**, 372 (2007).
[40] SIMION sold by Scientific Instruments Services Inc.
[41] R. H. Day, P. Lee, E. B. Saloman, and D. J. Nagel, J. Appl. Phys. **52**, 6965 (1981).
[42] Y. Lin and D. C. Joy, Surf. Interface Anal. **37**, 895 (2005).
[43] R. Gotter, F. Offi, A. Ruocco, F. Da Pieve, R. Bartynski, M. Cini, and G. Stefani, Europhys. Lett. **94**, 37008 (2011).
[44] M. Cini, E. Perfetto, R. Gotter, F. Offi, A. Ruocco, and G. Stefani, Phys. Rev. Lett. **107**, 217602 (2011).
[45] R. Gotter, G. Fratesi, R. A. Bartynski, F. Da Pieve, F. Offi, A. Ruocco, S. Ugenti, M. I. Trioni, G. P. Brivio, and G. Stefani, Phys. Rev. Lett. **109**, 126401 (2012).
[46] R. Gotter, M. Sbroscia, M. Caminale, S. R. Vaidya, E. Perfetto, R. Moroni, F. Bisio, S. Iacobucci, G. Di Filippo, F. Offi, A. Ruocco, G. Stefani, L. Mattera, and M. Cini, Phys. Rev. B **88**, 094403 (2013).
[47] I. S. Brandt, Z. Wei, F. O. Schumann, and J. Kirschner, Phys. Rev. B **92**, 155106 (2015).
[48] I. S. Brandt, Z. Wei, F. O. Schumann, and J. Kirschner, Phys. Rev. Lett. **113**, 107601 (2014).
[49] G. Baym, *Lecture On Quantum Mechanics* (Westview Press, Boulder, CO, 1969).
[50] R. L. Brown, Phys. Rev. A **1**, 586 (1970)
[51] W. Kohn, Rev. Mod. Phys. **71**, 1253 (1999).
[52] W. Kohn and L. J. Sham, Phys. Rev. **140**, A1133 (1965).
[53] N. Fominykh, J. Henk, J. Berakdar, P. Bruno, H. Gollisch, and R. Feder, Solid State Commun. **113**, 665 (2000).
[54] N. Fominykh, J. Berakdar, J. Henk, and P. Bruno, Phys. Rev. Lett. **89**, 086402 (2002).
[55] R. Feder and H. Gollisch, Solid State Commun. **119**, 625 (2001).
[56] R. Feder and H. Gollisch, in *Solid State Photoemission and Related Methods*, edited by W. Schattke and M. A. van Hove (Wiley-VCH, Weinheim, 2003), Chap. 9.
[57] H. Gollisch, N. v. Schwartzenberg, and R. Feder, Phys. Rev. B **74**, 075407 (2006).
[58] R. Feder, H. Gollisch, D. Meinert, T. Scheunemann, O. M. Artamonov, S. N. Samarin, and J. Kirschner, Phys. Rev. B **58**, 16418 (1998).
[59] H. Gollisch, X. Yi, T. Scheunemann, and R. Feder, J. Phys.: Condens. Matter **11**, 9555 (1999).
[60] J. Berakdar, H. Gollisch, and R. Feder, Solid State Commun. **112**, 587 (1999).